Nano Res (2010) 3: 452–458
DOI 10.1007/s12274-010-0006-8
Research Article

Aqueous Supercapacitors on Conductive Cotton

Mauro Pasta[1,2], Fabio La Mantia[2], Liangbing Hu[2], Heather Dawn Deshazer[2], and Yi Cui[2] (✉)

[1] Dipartimento di Chimica Inorganica, Metallorganica e Analitica "Lamberto Malatesta", Università degli Studi di Milano, Via Venezian 21, 20133 Milano, Italy

[2] Department of Materials Science and Engineering, Stanford University, Stanford, CA 94305, USA

Received: 17 March 2010 / Revised: 27 April 2010 / Accepted: 4 May 2010

ABSTRACT

Wearable electronics offer the combined advantages of both electronics and fabrics. In this article, we report the fabrication of wearable supercapacitors using cotton fabric as an essential component. Carbon nanotubes are conformally coated onto the cotton fibers, leading to a highly electrically conductive interconnecting network. The porous carbon nanotube coating functions as both active material and current collector in the supercapacitor. Aqueous lithium sulfate is used as the electrolyte in the devices, because it presents no safety concerns for human use. The supercapacitor shows high specific capacitance (~70–80 $F \cdot g^{-1}$ at 0.1 $A \cdot g^{-1}$) and cycling stability (negligible decay after 35,000 cycles). The extremely simple design and fabrication process make it applicable for providing power in practical electronic devices.

KEYWORDS

Supercapacitor, wearable electronics, energy storage, carbon nanotubes

1. Introduction

Wearable electronics constitute a new class of devices with an array of novel functionalities, which make them ideal for emerging applications such as high-performance sportswear, wearable displays, new classes of portable power, and embedded health monitoring devices [1–3]. All these electronic applications require light mass, wearable power conversion, and storage devices. Textiles are flexible and porous materials made by weaving or pressing natural or synthetic fibers, which gives them important properties such as flexibility, stretchability, and light mass. Thus, the ideal wearable power device would incorporate a textile as a component. Among textiles, cotton has the advantages of being an inexpensive natural fiber, which is highly hydrophilic and light.

In this work, we describe the conformal coating of single-walled carbon nanotubes (SWNTs) onto cellulose fibers to make porous conductors. The fabrication process is simple and scalable, similar to those widely used for dyeing fibers and fabrics in the textile industry. The SWNT coating makes these textiles highly conductive, with sheet resistance less than 1 $\Omega \cdot sq^{-1}$. The conductive textiles show outstanding mechanical and chemical properties. A thorough characterization of this material was recently reported [4], and can be referenced for specific details regarding physical properties. Specifically, the porous structure and high surface area make this material particularly interesting for supercapacitor applications. As an extension of our previous study, here we report the performance

Address correspondence to yicui@stanford.edu

of a symmetric SWNT/cotton supercapacitor in a safe aqueous electrolyte, whose components are fully compatible with wearable device applications.

2. Experimental

Sodium dodecylbenzene sulfonate (SDBS) and lithium sulfate anhydrous (≥ 99.99% trace metals basis) were purchased from Sigma Aldrich. Nitric acid (68%) was purchased from EMD Chemicals. Fluffy cotton sheets were purchased from Wal-Mart Stores, Inc.

Electrochemical characterization was carried out using a BioLogic VMP3 potentiostat/galvanostat multichannel equipped with an electrochemical impedance spectroscopy (EIS) board. A double junction Ag|AgCl|KCl (3.5 mol·L^{-1}) reference electrode (RE) was used in the measurements. The double junction was employed to prevent OH^- diffusion and reaction at the Ag/AgCl interface. In addition, the RE potential was monitored after each measurement to confirm that no change had taken place. All the measurements were performed under inert (nitrogen) atmosphere and at room temperature.

2.1 SWNT ink fabrication

10 mg·mL^{-1} SDBS surfactant was dissolved in deionized (DI) water with the help of bath sonication. Laser ablation SWNTs were then dispersed in the surfactant solution to a concentration of 1.6 mg·mL^{-1}. After bath sonication for 5 min, the SWCNT dispersion was probe-sonicated for 30 min at 200 W (VC 505, Sonics Inc).

2.2 SWNT/cotton preparation procedure

A fluffy cotton sheet with thickness of ~1–2 mm was dipped into the SWNT ink and immediately removed. Due to the strong absorption, the ink quickly coated the textile. The textile with SWNT ink was subsequently dried in an oven at 120 °C for 10 min to remove water. The mass of the SWNTs was obtained from the mass difference before and after the dipping and drying of the cotton sheet. This process was repeated to increase the SWNT loading in the cotton. Figure 1 shows the accumulated ink mass absorbed per cm^2 of the cotton after different numbers of dipping and drying cycles. A small variation (<5%) of absorbed ink mass per area was observed when repeating the process.

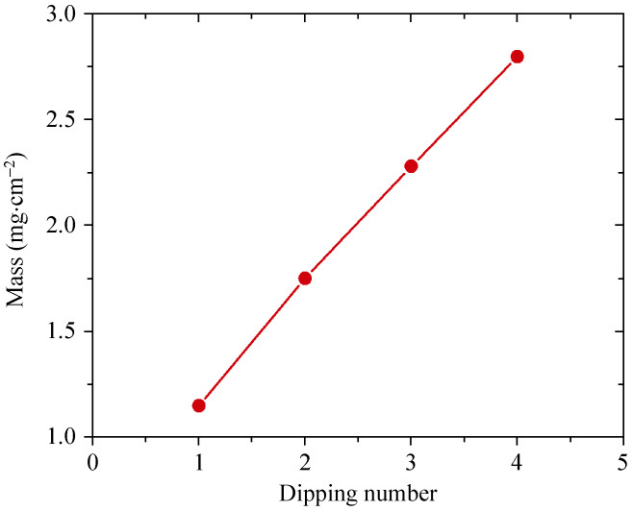

Figure 1 The amount of ink absorbed per area by the cotton sheet after dipping for different numbers of times

The cotton fiber structure is comprised of multiple individual cotton fibrils, which are in turn composed of multiple microfibrils, bundled together. The microfibrils are made of poly-*D*-glucose chains, usually arranged in crystalline, or partially crystalline, domains. This structure allows the fibers to absorb large amounts of water, or other polar solvents.

The scanning electron microscope (SEM) image in Fig. 2(b) reveals the macroporous structure of a cotton sheet and Fig. 2(c) shows the conformal coating of SWNTs onto the fibers. This conformal coating is a result of the mechanical flexibility of the individual SWNTs and the strong binding energy between SWNTs and cotton fibers [5], accounting also for the high electrical conductivity of the textile. Previous studies have shown that SWNT films have microscale porosity, which is required to maximize the specific capacitance [6]. The microporous structure on top of the macroporous textile leads to what we call a "double porous structure" that facilitates the easy access of electrolyte ions to the SWNTs, which is essential for high power supercapacitor applications. Transmission electron microscopy (TEM) images of the SWNT/cotton fibers (Fig. 2(d)) show that the SWNTs are well bonded to the fiber, forming a cross-linked network, which provides conducting pathways.

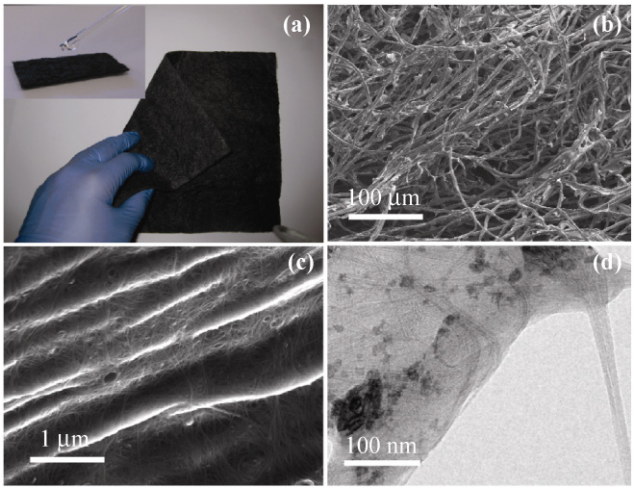

Figure 2 (a) A 15 cm × 15 cm foldable textile conductor based on a cotton sheet with sheet resistance of 2 $\Omega \cdot sq^{-1}$. The water drop test on the SWNT-coated cotton shows the highly hydrophilic surface. (b) SEM image of the cotton sheet coated with SWNTs. (c) Higher magnification image of the sample in (b) showing the conformal coating of SWCNTs on the cotton surface. (d) TEM image of SWNTs on a cotton fiber demonstrating that there is no evidence of agglomeration of SWNTs

Such porous textile conductors demonstrate excellent electrical, mechanical, and chemical resistance performance [4] suggesting that the SWNTs adhere very strongly to the cotton fibers, which is critical for wearable electronic and power devices. Such strong binding may be due to the following:

1) There are strong van der Waals forces existing between SWNTs and the textile fibers [5].

2) Acid-treated SWNTs have carboxyl functional groups on the surfaces and the ends, which can form strong hydrogen bonds with the hydroxyl groups in the cellulose fibers.

3) The flexibility of SWNTs allows them to conformally adhere to the surface of cotton fibers, maximizing the surface contact area between SWNTs and textile fibers [7].

The superior mechanical adhesion of SWNTs on cotton (measured by the standard tape test and by washing in water) is essential for high-speed roll-to-roll fabrication and energy storage device stability.

2.3 Surfactant removal

The material prepared as described above is highly hydrophilic, due to the surfactant still present on the surface. However, this surfactant needs to be removed to avoid side reactions, which would generate irreversible specific charge and self-discharge phenomena. The surfactant removal is essential for the final device performance, especially its cyclability and coulombic efficiency. Washing with abundant DI water and pressing with a grid are sufficient to remove the surfactant. A simple rule of thumb to evaluate whether all the surfactants have been removed is to press the fabric and see if bubbles are produced.

2.4 SWCNT/cotton pretreatment

After the SDBS removal, the textile exhibits a hydrophobic behavior which is incompatible with its application in a water-based electrolyte. To improve the surface hydrophilicity and remove the last traces of surfactant, the textile was dipped into a 4 $mol \cdot L^{-1}$ HNO_3 solution for about 6 h and then washed again with DI water to remove the acid. Treating the nanotubes with nitric acid introduces a larger number of oxygen-containing functional groups such as carboxyl, lactones, and phenols and creates a more hydrophilic surface structure [8]. The nitric acid treatment also has two other advantages: it helps to remove impurities, such as catalytic metal particles responsible for self discharge problems [9] and induces hole doping, which decreases the resistivity of the nanotubes [10–12]. Figure 2(a) shows the results of wettability tests of the substrate after the acid treatment.

As mentioned above, the acid wash is also the final step in the surfactant removal process. To confirm the success of the washing process in removing all the surfactants it is sufficient to observe the open circuit voltage value against the RE. If the value lies around 0.0 V vs. RE, this means that there is still some surfactant left, and it is necessary to repeat the washing process. The observed open circuit voltage is due to an unidentified secondary reaction involving the surfactant. If the value lies around 0.4 V vs. RE, we can be sure that all the surfactants have been eliminated and proceed with the electrochemical tests.

2.5 Electrochemical tests

The performances of the prepared SWCNT/cotton electrodes were tested in an aqueous 2 $mol \cdot L^{-1}$ Li_2SO_4

solution. This electrolyte was chosen for the following reasons:

1) Sulfates combine the advantages of electrochemical stability in the potential range investigated, with low cost.

2) Among the sulfates, lithium sulfate has the advantage of a higher solubility in water, as compared to the less expensive sodium and potassium salts.

3) A 2 mol·L^{-1} solution of lithium sulfate has an acidic pH (around 3.2); a slow H_3O^+ ion sorption has been reported in the literature, giving an additional capacity [13].

Before each measurement the electrolyte was purged with nitrogen gas for 30 min to remove the dissolved oxygen which could give rise to an irreversible specific charge. All the measurements were performed under nitrogen atmosphere.

3. Results and discussion

Figure 3 reports galvanic cycles (100 μA·cm^{-2}) for SWCNT/cotton materials with four different SWCNT loadings (0.12, 0.24, 0.36, 0.47 mg·cm^{-2}) corresponding to one to four "dip and dry" cycles, referred to as cotton #1, #2, #3, #4, respectively. As one can observe, the specific charge (represented by the area underneath the curves) increases with the SWCNT loading.

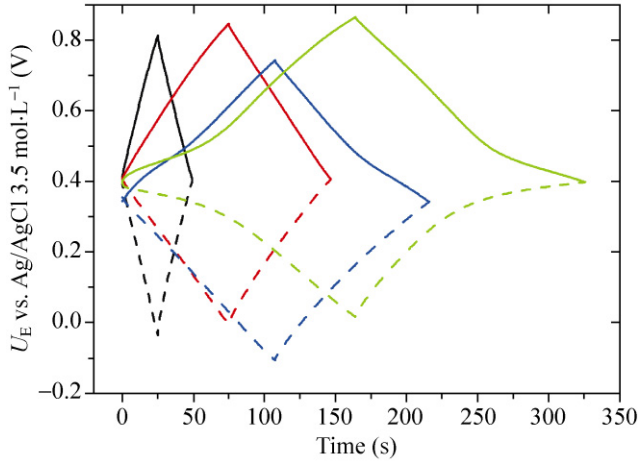

Figure 3 Galvanostatic cycling at apparent current density of 0.1 mA·cm^{-2} for working (continuous lines) and counter (dotted lines) SWNT/cotton electrodes vs. Ag/AgCl 3.5 mol·L^{-1} in 2 mol·L^{-1} Li_2SO_4 electrolyte, for different mass loadings of SWNTs. Black curve: cotton #1 (0.12 mg·cm^{-2}); red curve: cotton #2 (0.24 mg·cm^{-2}); blue curve: cotton #3 (0.36 mg·cm^{-2}); green curve: cotton #4 (0.47 mg·cm^{-2})

In the presence of an RE, the behavior of both positive and negative electrodes can be monitored during the cycling. With this approach some irreversible behavior in the cathodic side can be easily identified during the first few cycles: the reason is the low hydrogen evolution overpotential on SWCNTs, as already reported in Ref. [13]. Moreover, the shape of the curve—especially the one for high SWCNT loadings—suggests the presence of a slow ion sorption, leading to an additional specific charge at lower specific currents. Ion sorption is a process that allows more charge to accumulate in the inner Helmholtz layer, but it is normally a slow process (time constant >10^{-6} s) with respect to the accumulation of charge in the outer Helmholtz layer (time constant <10^{-10} s). Therefore, it can only be observed at low scan rates.

In order to thoroughly investigate this phenomenon, the differential curves, obtained by taking the derivative of the charge Q with respect to the electrode potential U_E, are reported in Fig. 4 for a current intensity of 100 μA. We want to stress that at higher mass loading (lower specific current) a peak appears in the positive electrode of the supercapacitor around 0.4 V vs. Ag/AgCl 3.5 mol·L^{-1}. This peak is evidence of an electrochemical adsorption or an ion sorption process, as described above.

The electrochemical adsorption/ion sorption is even more evident in the Nyquist plots (Fig. 5) of the EIS performed on the electrodes. From the shape of the

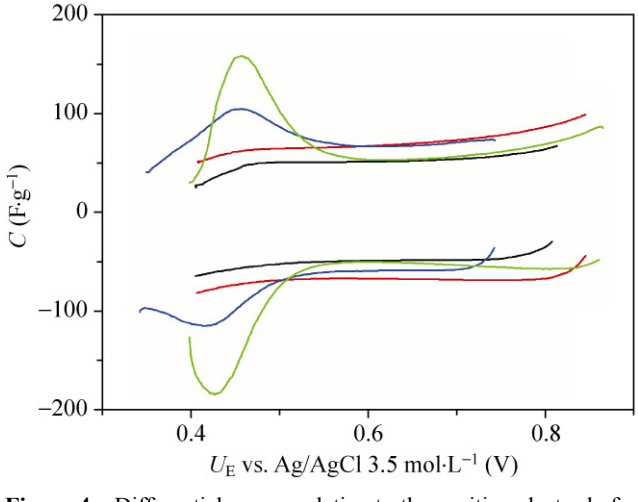

Figure 4 Differential curves relative to the positive electrode for different SWNT loadings. Black curve: cotton #1 (0.12 mg·cm^{-2}); red curve: cotton #2 (0.24 mg·cm^{-2}); blue curve: cotton #3 (0.36 mg·cm^{-2}); green curve: cotton #4 (0.47 mg·cm^{-2})

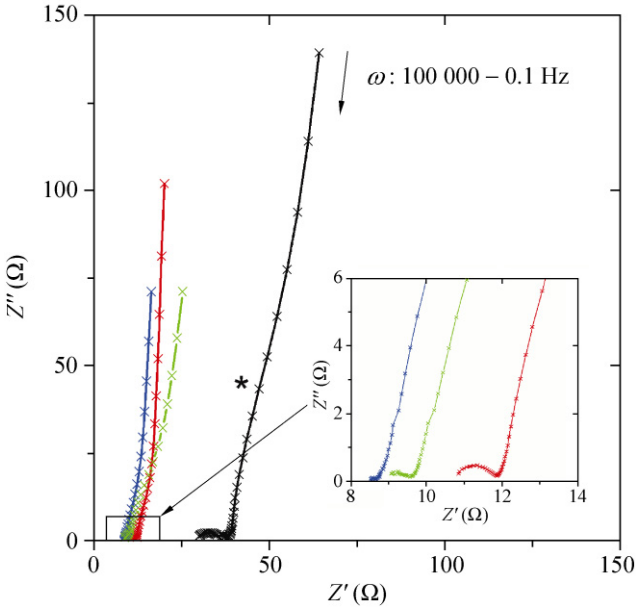

Figure 5 Nyquist plots for supercapacitors with different SWNT loadings. Black curve: cotton #1 (0.12 mg·cm^{-2}); red curve: cotton #2 (0.24 mg·cm^{-2}); blue curve: cotton #3 (0.36 mg·cm^{-2}); green curve: cotton #4 (0.47 mg·cm^{-2})

Nyquist plot and the value of the impedance at different mass loadings, we can obtain the following information:

1) The distorted capacitive semicircle at high frequencies (see insert in Fig. 5) is evidence of a current distribution along the thickness of the electrode and of an electrochemical process which is different from simple double layer charging/discharging [14–16].

2) The increase in the capacitive part of the impedance after the high-frequency semicircle is due to the blocking nature of the electrochemical process, thus, indicating that it is an electrochemical adsorption or an ion sorption.

3) The small difference in the value of the imaginary part of the impedance at low frequencies between the different mass loadings suggests that the electrochemical process is limited by the transport of the adsorbed species in the pores. Also, the inflection point (*) at low frequencies is indicative of such a phenomenon.

4) After reaching a mass loading of 0.24 mg·cm^{-2}, the internal resistance of the supercapacitor is due to the transport of ions in the electrolyte.

There are four main species in solution: Li^+, SO_4^{2-}, H_3O^+, and OH^-. The Li^+ and SO_4^{2-} ions are present in such high concentrations that their ion sorption should not be transport limited. OH^- is present in such a low concentration that it is unable to account for the specific charge under the peak in Fig. 4 (green curve). Thus, it can be concluded that hydronium (H_3O^+) ion sorption is responsible for the EIS behavior.

Figure 6 shows the specific capacitances at various specific currents. The curve representing the lowest SWCNT content (cotton #1) shows the worst performances in terms of both specific capacitance (55 F·g^{-1}) and capacitance retention at higher specific currents: this behavior is due to the low electrical conductivity of the substrate (as also indicated by the Nyquist plot, Fig. 5). At this mass loading, the SWCNT content is insufficient to form a good interconnecting network. For cotton #2, the specific capacitance is higher, with a maximum value of about 70 F·g^{-1}, and it is relatively constant in the current range from 10 μA·g^{-1} to 1 mA·g^{-1}. Comparing cotton #2 and cotton #3, it is found that the performances are quite similar, in terms of maximum specific capacitance, but the specific capacitance decreases more rapidly at higher current values for cotton #3. For cotton #4 the maximum specific capacitance is higher (around 80 F·g^{-1}), but it continuously decreases with increasing current. This behavior can be interpreted by using the framework of the theory of current density distribution in porous

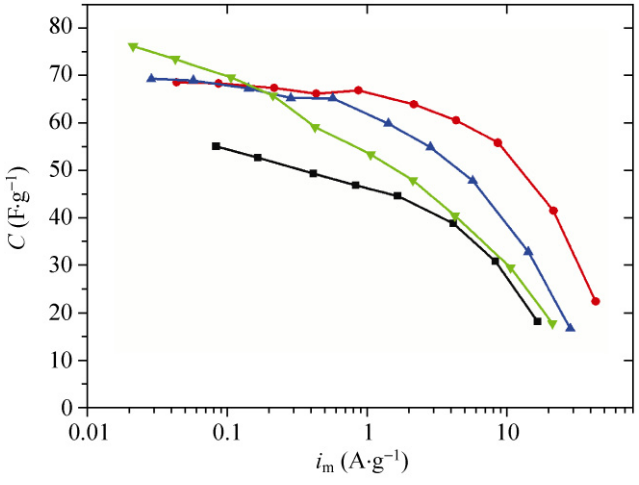

Figure 6 Plots of specific capacitance versus specific current for SWNT/cotton electrodes with different SWNT loadings. Black curve: cotton #1 (0.12 mg·cm^{-2}); red curve: cotton #2 (0.24 mg·cm^{-2}); blue curve: cotton #3 (0.36 mg·cm^{-2}); green curve: cotton #4 (0.47 mg·cm^{-2})

electrodes. This theory can be summarized by the following equation [17]:

$$\frac{\partial^2 \Delta \Phi}{\partial x^2} = \frac{\rho_s I}{af} \quad (1)$$

where $\Delta\Phi$ is the potential drop at the solid/liquid interface, x represents the position within the porous electrode, ρ_s is the resistivity of the electrolyte solution, a the characteristic length of the porous electrode, f the void fraction, and I the current density at the solid/liquid interface (which is dependent on the position x). The characteristic length, a, increases on increasing the ratio between the volume of the electrode and the active surface area, V/A. Equation (1) is valid when the electric resistance of the solid phase in the porous electrode is negligible. The behavior of the electrodes at different current densities is better understood when the areal capacitance (capacitance per geometrical area) with respect to the mass loading is reported (see Fig. 7). When the apparent current density (the current density per geometrical area) is low (black curve), Eq. (1) reduces to a constant current density distribution along the pores of the electrode, and therefore, the areal capacitance increases linearly with the mass loading. At higher apparent current densities (the red, blue, and green curves in Fig. 7), the electrodes with a larger a value (lower mass loading) still charge homogeneously, while ones with lower a (higher mass loading) show a distribution of current density, and consequently a distribution of surface charge. As observed in Fig. 7 for the red, blue, and green curves, the higher the apparent current density, the stronger the deviation from linearity. The deviation from linearity always leads to a reduction in the areal capacitance. Depending on the application, the optimal loading is easily predicted.

The cycling stability of the SWNT/cotton#2 device was tested at room temperature, under a nitrogen atmosphere with a three electrode configuration cell, as shown in Fig. 8. The electrolyte used was 2 mol·L^{-1} Li_2SO_4 and the experiment was performed with an apparent current density of 1 mA·cm^{-2}. No fading was observed after 35,000 cycles. The coulombic efficiency after 35,000 cycles was higher than 99% of the initial value, with the specific capacitance being around 45 F·g^{-1}.

4. Conclusions

A supercapacitor has been fabricated using a conformally coated SWNT/cotton fabric as both active material and current collector (resistance lower than 1 Ω·sq^{-1}). The device has excellent cycling performance (good capacity retention after 35,000 cycles) and high

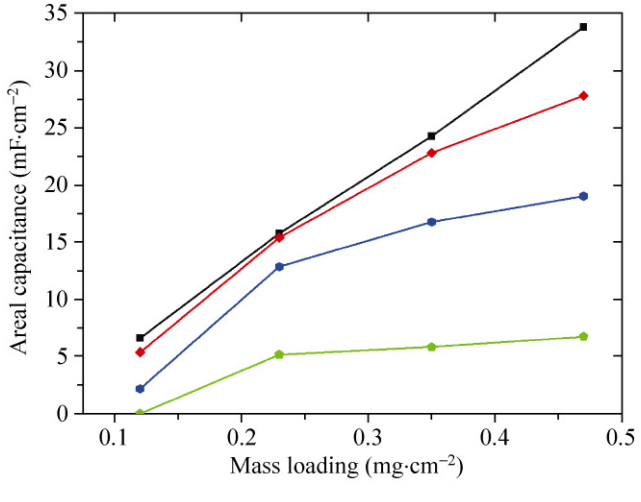

Figure 7 Plots of areal capacitance versus mass loading for different apparent current densities. Black curve; 0.01 mA·cm^{-2}; red curve: 0.2 mA·cm^{-2}; blue curve: 2 mA·cm^{-2}; green curve: 10 mA·cm^{-2}

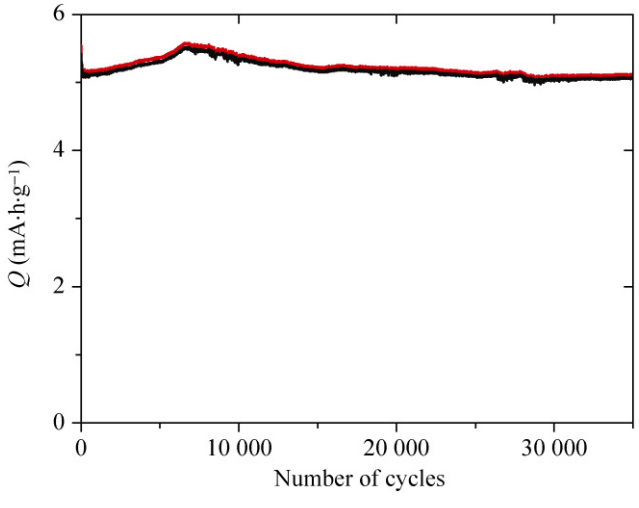

Figure 8 Cycling stability of SWNT/cotton #2 supercapacitor device in 2 mol·L^{-1} Li_2SO_4 aqueous electrolyte at 1 mA·cm^{-2} apparent current density

specific capacitance (70–80 $F \cdot g^{-1}$ at 0.1 $mA \cdot cm^{-2}$). The device as prepared is fully wearable since both the textile (cotton) and the lithium sulfate electrolyte are compatible with the human body. It can also be integrated into wearable devices. By means of impedance spectroscopy and differential curves, we have highlighted an additional reversible capacitance due to a slow ion sorption process.

Potential improvements in the future need to be directed towards an asymmetric supercapacitor since the hydrogen evolution overpotential limits the operative voltage range, and therefore the high power limit.

Acknowledgements

Y. C. acknowledges support from the King Abdullah University of Science and Technology (KAUST) Investigator Award (No. KUS-l1-001-12).

References

[1] Gniotek, K.; Krucińska, I. The basic problems of textronics. *Fibres Text. East. Eur.* **2004**, *12*, 13–16.

[2] Lukowicz, P.; Kirstein, T.; Troster, G. Wearable systems for health care applications. *Method. Inform. Med.* **2004**, *43*, 232–238.

[3] Park, S.; Jayaraman, S. Smart textiles: Wearable electronic systems. *MRS Bull.* **2003**, *28*, 585–591.

[4] Hu, L.; Pasta, M.; La Mantia, F.; Cui, L.; Jeong, S.; Deshazer, H. D.; Choi, J. W.; Han, S. M.; Cui, Y. Stretchable, porous, and conductive energy textiles. *Nano Lett.* **2010**, *10*, 708–714.

[5] Hertel, T.; Walkup, R. E.; Avouris, P. Deformation of carbon nanotubes by surface van der Waals forces. *Phys. Rev. B* **1998**, *58*, 13870–13873.

[6] An, K. H.; Kim, W. S.; Park, Y. S.; Choi, Y. C.; Lee, S. M.; Chung, D. C.; Bae, D. J.; Lim, S. C.; Lee, Y. H. Supercapacitors using single-walled carbon nanotube electrodes. *Adv. Mater.* **2001**, *13*, 497–500.

[7] Iijima, S.; Brabec, C.; Maiti, A.; Bernholc, J. Structural flexibility of carbon nanotubes. *J. Chem. Phys.* **1996**, *104*, 2089–2092.

[8] Yu, X.; Lin, B.; Gong, B.; Lin, J.; Wang, R.; Wei, K. Effect of nitric acid treatment on carbon nanotubes (CNTs)-cordierite monoliths supported ruthenium catalysts for ammonia synthesis. *Catal. Lett.* **2008**, *124*, 168–173.

[9] Tohji, K.; Goto, T.; Takahashi, H.; Shinoda, Y.; Shimizu, N.; Jeyadevan, B.; Matsuoka, I.; Saito, Y.; Kasuya, A.; Ohsuna, T.; Hiraga, K.; Nisshina, Y. Purifying single-walled nanotubes. *Nature* **1996**, *383*, 679.

[10] Parekh, B. B.; Fanchini, G.; Eda, G.; Chhowalla, M. Improved conductivity of transparent single-wall carbon nanotube thin films via stable postdeposition functionalization. *Appl. Phys. Lett.* **2007**, *90*, 121913.

[11] Zhou, W.; Vavro, J.; Nemes, N. M.; Fischer, J. E.; Borondics, F.; Kamaras, K.; Tanner, D. B. Charge transfer and Fermi level shift in p-doped single-walled carbon nanotubes. *Phys. Rev. B* **2005**, *71*, 205423.

[12] Beaudrouet, E.; Le Gal La Salle, A.; Guyomard, D. Nanostructured manganese dioxides: Synthesis and properties as supercapacitor electrode materials. *Electrochim. Acta* **2009**, *54*, 1240–1248.

[13] Prosini, P. P.; Pozio, A.; Botti, S.; Ciardi, R. Electrochemical studies of hydrogen evolution, storage and oxidation on carbon nanotube electrodes. *J. Power Sources* 2003, *118*, 265–269.

[14] Newman, J. S.; Tobias, C. W. J Theoretical analysis of current distribution in porous electrodes. *Electrochem. Soc.* **1962**, *109*, 1183–1191.

[15] de Levie, R. Porous electrodes in electrolyte solutions. Ⅳ. *Electrochim. Acta* **1964**, *9*, 1231.

[16] Ng, S. H.; La Mantia, F.; Novak, P. A multiple working electrode for electrochemical cells: A tool for current density distribution studies. *Angew. Chem. Int. Ed.* **2009**, *48*, 528–532.

[17] Daniel-Bek, V. S. Polarization of porous electrodes. I. Distribution of current and potential within an electrode. *Zh. Fiz. Khim.* **1948**, *22*, 697–710.